Chapter 2. Semiconductor Surface Studies

Academic and Research Staff

Professor John D. Joannopoulos, Professor Tomas A. Arias, Dr. Karl Brommer

Graduate Students

Rodrigo B. Capaz, Kyeongjae Cho

Technical and Support Staff

Imadiel Ariel

2.1 Introduction

Understanding the properties of surfaces of solids and the interactions of atoms and molecules with surfaces is extremely important both from the technological and academic points of view. The advent of ultrahigh vacuum technology has made microscopic studies of well-characterized surface systems possible. The way atoms move to reduce the energy of the surface, the number of layers of atoms involved in this reduction, the electronic and vibrational states that result from this movement, and the final symmetry of the surface layer are all of utmost importance in arriving at a fundamental and microscopic understanding of the nature of clean surfaces, chemisorption processes, and the initial stages of interface formation.

The theoretical problems associated with these systems are quite complex. However, we are currently at the forefront of solving the properties of real surface systems. In particular, we are continuing our efforts to develop new techniques for calculating the total ground-state energy of a surface system from "first principles," so that we can provide accurate theoretical predictions of surface geometries and behavior. Our efforts in this program have concentrated in the areas of surface growth, surface reconstruction geometries, structural phase transitions, and chemisorption.

2.2 Chemisorption

In this section we discuss an *ab initio* theoretical investigation of the electronic surface states and the reactivity of the Si(111)-(7x7) surface reconstruction. The Si(111)-(7x7) reconstruction has a rich and complex chemistry because it contains a diverse set of dangling bonds. This surface is a challenge for studying surface reactions, because a single atomic species reconstructs into a large (7x7) unit cell containing nineteen dangling bonds. The nineteen dangling bonds in the unit cell define nineteen different reactive sites, each on a silicon atom. Seven are unique, with the other twelve related by symmetry. It is difficult and challenging to rationalize the dramatic differences in reactivity among the different sites on the surface. While this reconstruction has been studied for thirty years, it is only with the use of massively parallel computers that realistic *ab initio* studies of its electronic structure are tractable. In particular, we used the *ab initio* molecular dynamics scheme that we have developed at MIT for calculating the electronic states and computing the relaxed positions of the ions.

The relaxed positions of atoms in the 7x7 unit cell are plotted in figure 1. A top view of the surface with the unit cell outlined with dotted lines is shown in figure 1a. In this figure, all unique dangling
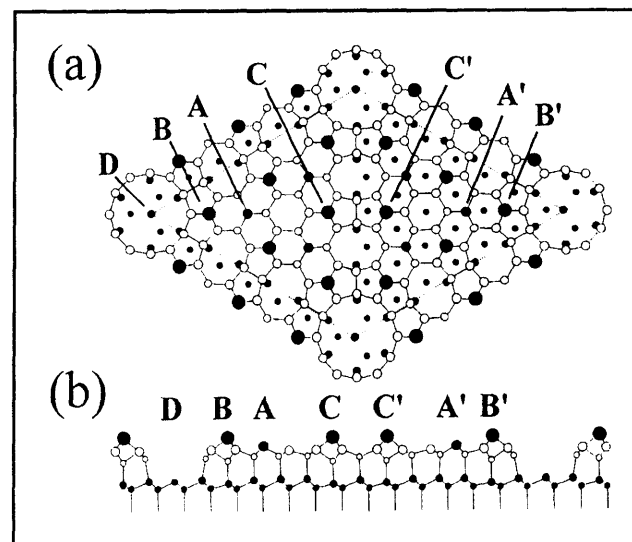

Figure 1. Si(111)-(7x7) surface dangling bond sites.

bonds are labeled with capital letters. The faulted and unfaulted rest atoms, denoted by shaded circles labeled A and A' respectively, sit on the top surface bilayers. There are a total of six rest atoms, three on each side of the unit cell. The large black circles labeled B, B', C and C' denote adatoms sitting on the top of the first surface bilayer. The six adatoms on each side of the unit cell form triangles. Adatoms at the faulted and unfaulted triangle corners B and B' are chemically distinct from adatoms at the triangle centers C and C'. The relative heights of the surface atoms are plotted in figure 1b, showing a side view through the long diagonal of the cell. It can be seen that the rest atoms with the dangling bonds are buckled slightly upward from the positions of other first-layer atoms. In the side view, the depth of the large hole at each corner of the cell is also apparent. Inside this corner hole sits the nineteenth dangling bond site, labeled D.

Surface chemisorption will depend on a variety of factors, especially electronic effects dictating the existence and magnitude and activation barriers, as well as dissipative channels for the energy of incident reactants, steric constraints, and surface diffusion. The close similarity of different dangling bonds sites on the complex Si(111)-(7x7) surface reconstruction means that most of the common chemisorption factors are virtually identical among the different sites. To determine reactivity we construct a theory that is based on two parameters describing the electronic surface states: the global electronegativity, and the local softness.

The definition of local softness introduced by Yang and Parr for metals was extended to systems with a gap to obtain regional softness for the Si(111)-(7x7) surface reconstruction. Two different classes of regional softness are calculated, one related to the nucleophilic (acceptor) capacity, and the other related to the electroophilic (acceptor) capacity of the surface. Accordingly, an order can be assigned for the nucleophilic and electrophilic nature of the seven dangling bonds of the surface. From this analysis of regional softness, a general qualitative behavior for the reactivity of this surface reconstruction can emerge.

For our application, we are interested in determining the possible differences in reactivity between the seven types of dangling bonds in the system. To do this we defined a regional reactivity index associated with a local region of the surface through spatial integration of the local softness

$$S_i = \int_{\Omega_i} s(r)\, dr,$$

where Ω_i is the local volume surrounding the dangling bond i. As an extension of the physical meaning of s(r) we interpret S_i as the measure of the ability of the dangling bond i to perform charge transfer. Extrapolating from Politzer, we choose the name *charge capacity* for this property. Thus, differences in charge transfer capabilities among the different dangling bonds will be determined entirely through S_i.

Our calculations of the charge capacity, S_i are exhibited in figure 2. An analysis of the values in this figure shows that the donor and acceptor capacities follow the order displayed in table 1. Table 2 summarizes the differences in charge capacity between faulted and unfaulted halves of the unit cell.
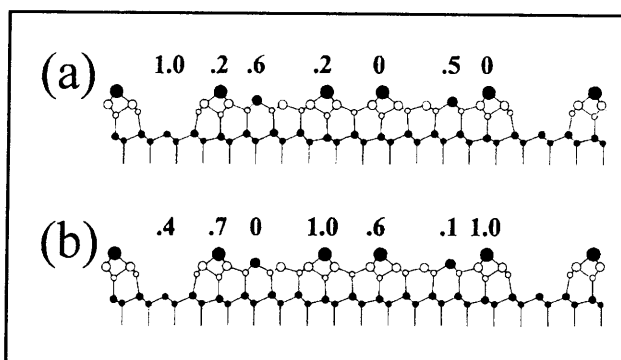

Figure 2. Charge capacity of each unique dangling bond on the 7x7 surface for (a) electrophilic and (b) necleophilic reactants.

Table 1. Charge capacity order for different sites on the Si(111)-(7x7) reconstruction	
Surface donor capacity	Corner hole > rest atoms > adatoms
Surface acceptor capacity	Adatoms > corner hole > rest atoms

Table 2. Differences in charge capacity between faulted and unfaulted halves	
As a donor	Faulted rest atoms > unfaulted rest atoms
As an acceptor	Faulted center adatoms > unfaulted center adatom Unfaulted corner adatoms > faulted corner adatom

General reactivity patterns. According to table 1, electrophilic attaching groups interact with the surface in the following order: corner hole > rest atom > adatoms. The corner hole and rest atom

reactivities are strong, while the adatom reactivity is relatively weak. The nucleophilic groups interact with the surface mainly through the adatoms, to a lesser extent with corner holes, and most weakly with the rest atoms. Among the seven different dangling bonds the corner holes is unique in exhibiting a strongly active site for electrophilic reactants as well as exhibiting some reactivity for nucleophilic reactants. Adatoms are more selective towards nucleopholes. While rest atoms are strongly reactive toward electrophilic species, the rest atoms are weakly reactive toward necleophilic species.

We now consider the effects of the stacking fault in the reactivity of the Si(111)-(7x7) reconstruction. With respect to donor capacity, there is a clear distinction between reactivity at faulted and unfaulted halves as shown in table 2. Electrophiles should prefer to interact with the faulted half of the surface, and in particular with the faulted rest atoms. With respect to acceptor capacity, there does not appear as strong a selectivity for one half or the other since preferred reactive sites are found on both sides to the unit cell. If a donor (nucleophile) reacts with the faulted half, the interaction will be primarily with the faulted center adatom. If the unfaulted half is selected, the interaction is generally with the unfaulted corner adatom.

Reactions preserving reconstruction. To illustrate the utility of the present approach, we will use it to analyze some experimental reactivity patters of the Si(111)-(7x7) reconstruction. In particular, table 3 displays the reactivity patterns for some attacking compounds which maintain the reconstruction. The experimental information was obtained using infrared spectroscopic techniques by Chabal and by scanning tunneling microscopy (STM) by Avouris and colleagues. To classify the reactants as donors or acceptors, we used an electronegativity criterion. If the difference in electronegativity between the surface and the reactant is negative, then the reactant is the acceptor and the surface the donor. If the difference is positive, the roles are reversed. Table 4 shows these differences for a series of compounds. Electronegativities for the reactants were taken from Pearson's estimations. The surface electronegativity is the work function, 4.8 eV.

Interaction with hydrogen. According to table 4, H can be classified as an acceptor species with respect to the surface. Hydrogen is one of the most electronegative of the neutral reactants listed in this table. From table 4 it is clear that the corner hole atoms are the most reactive sites in this case, and this is in complete agreement with the experiments of Chabal et al. summarized in table 3.

Table 3. Experimental studies of chemical reactivity of the Si(111)-(7x7) reconstruction		
Reactant	Method	Reactivity
H	Spectroscopy	The most active site is the corner hole atom
Pd, Ag, Li	STM	The faulted half is preferred and reactants are believed to bond primarily to rest atoms and center adatoms
NH_3, H_2O, PH_3	STM	Rest atoms > center adatoms > corner adatoms

Interaction with Pd, Ag, and Li. According to table 4, these metal atoms are electron donors with respect to the surface. Thus, our theoretical calculations suggest that they should interact primarily with adatoms and specifically with faulted center adatoms. This is again consistent with the experimental evidence summarized in table 3.

Interaction with NH_3, H_2O, *and* PH_3. These molecules dissociate on the surface into anions OH^-, $(NH_2)^-$, and $(PH_2)^-$ and the cation H^+. From table 4, all of the dissociation products except the proton are donors. The proton is clearly a strong acceptor. By assuming that the dissociation process takes place in the initial step of the reaction without inducing large changes in the chemical potential of the surface, we determine the order of preferential reactivity as corner hole atoms, then rest atoms, and last adatoms. Table 3 shows that the predicted reactivity order of rest atoms and adatoms agrees with experimental STM data. Our calculations also predict that the corner hole site is the most reactive. This remains to be detected experimentally, but may be difficult due to the depth of the corner hole below the adatom and rest atom layers.

Interaction with O_2. From table 4, the O_2 molecule is an electron acceptor with respect to the Si surface. Therefore, it should prefer to interact with the faulted half of the unit cell. Our calculations predict that the corner hole is the preferred reaction site, followed by rest atoms and adatoms. The preference for the faulted half agrees with STM experiments. Room temperature experiments have shown that O_2 is a molecular precursor which then dissociates and reacts preferentially with corner adatoms compared to center adatoms. While the regional softness of the isolated Si surface explains the preference for the faulted half by the molecular precursor, the presence of O_2 on the surface changes the local softness sufficiently to require

recomputation of local softness to analyze reactivity after dissociation.

Table 4. Relative electronegativity of reactants	
Reactant	Electronegativity difference (eV)
Li	1.8
Ag	0.4
Pd	0.3
PH₃	0.7
H	-2.4
NH₃	2.2
H₂O	1.7
Radicals (anions)	
NH₂	-1.3
OH	-2.7
PH₂	-0.7
Acceptors	
As	-0.5
Au	-1.0
Pt	-0.8
Metal cations	<0.0
Halgen atoms	<0.0
BF₃	-1.4
H₂	-1.9
O₂	-1.5
Donors	
Ga	1.6
Pb	0.9
Al	1.6
Ti	1.3
Alkaline Metals	>0.0

Predicted interactions. Based on the success of our reactivity analysis as demonstrated in the preceding example, we attempt to predict the reactivity associated with a number of atoms and molecules that yet remain to be studied. By using Pearson's electronegativity tables and the work function of the surface, we can classify a great variety of atoms and molecules as donors or acceptors with respect to the Si(111)-(7x7) reconstruction. Selected examples are presented in table 5 including predictions of possible reaction patterns. These examples were chosen to illustrate the interaction of both acceptors and donors with the surface, including both hard and soft chemical reactants. The predictions assume non dissociative interactions and that surface reconstruction is maintained.

Table 5. Theoretical predictions of the chemical reactivity of the Si(111)-(7x7) reconstruction	
Reactant	Reactivity
Acceptors: As, Au, Pt, metal cations, halogens, BF₃, H₂	Corner hole > rest atoms > adatoms

Faulted rest atom > unfaulted rest atom |
| Donors: Ga, Pb, Al, Ti, Ca, alkaline metals | Adatoms > corner holes > rest atoms

Faulted center adatoms > faulted corner adatoms |

2.3 Cross-sectional Scanning Tunneling Microscopy

Scanning tunneling microscopy (STM) provides an image of the structure of a surface at atomic resolution. This STM image is generated by an electron tunneling between the STM tip and a surface atom under the tip as a result of the overlap between the tip and surface wave functions. Consequently, the tip and the surface may in certain cases interact significantly during the process of an STM measurement. The conventional theories of STM, however, are based on a first order perturbation approximation which does not include the tip-surface interaction. STM images are then interpreted simply as a convolution of the tip wave function and the surface wave function. Although this interpretation is a very useful approximation for many applications, there may exist systems for which the tip-surface interaction and the surface dynamics play a crucial role in the STM measurement process.

In this section we describe *ab initio* total energy pseudopotential calculations to demonstrate that the Si(100) surface is an example of a system for which STM does not provide a direct mapping of

the surface atomic structure and that a conventional interpretation of the STM images is not appropriate. Typically, a room temperature STM image of the Si(100) surface shows the majority of dimers in what appear to be unbuckled, symmetric configurations. Such configurations are in disagreement with the theoretical predictions of buckled, asymmetric dimer configurations. One might expect that this discrepancy could reasonably be resolved by arguing that thermal fluctuations in the asymmetric dimer configurations will create an averaged or "symmetric" image. Such thermal fluctuations have been predicted to be present on the surface in the absence of a tip. In the presence of a tip, however, we propose that a different mechanism is operational. Specifically, we demonstrate that the tip-surface interactions are significant enough to flip and bind an asymmetric dimer to the tip. As the tip is then moved along the surface, dimers are flipped tracking the tip and create what appears to be a symmetric image in the scan.

In our calculations, we allowed the tip to vary in the range 4.5 to 5.2 Å above the atoms in the outermost surface layer. As shown in figure 3 even for the shortest tip-surface distance of 4.5 Å, the surface is not greatly perturbed by the presence of the tip, and no new bonds are formed between them. Nevertheless, as we discuss in the next section, there is enough interaction between tip and surface to significantly alter the dynamics of the surface dimers.

Figure 3. This plot shows a cross section of the total charge density of the tip-surface system with the tip directly above an upper dimer atom. The buckling angle of the dimer, the position of the apex tip atom, and the charge density distributions of the tip and the dimer are not significantly changed by the tip-surface interaction, but the intereaction energy is significant. (- 0.57 eV).

Interaction energies. The tip-surface interaction energy is calculated by combining three separately calculated energies: E(tip), E(surface), and E(tip+surface). The results of our calculations for a tip restricted to lie directly above a surface atom are summarized in figure 4. For the configuration shown on the left panel, the tip lies 5.2 Å above the lower dimer atom, and the interaction energy is -0.37 eV. The panel at the center of the figure refers to a symmetric dimer configuration that corresponds to the "saddle point" or static barrier configuration for flipping the buckled dimer. In the absence of the tip, the barrier is calculated to be 0.08 eV in good agreement with 0.09 eV as obtained by Dabrowski and Scheffler. In the presence of the tip, the barrier for an *up flip* of the buckled dimer is found to be 0.1 eV. The opposite barrier, corresponding to a down flip of the buckled dimer is obtained from the right panel of figure 4 and is found to be 0.3 eV. Note that the interaction energy in the latter case is correspondingly large at -0.57 eV and the distance between tip and dimer atom is 4.5 Å.
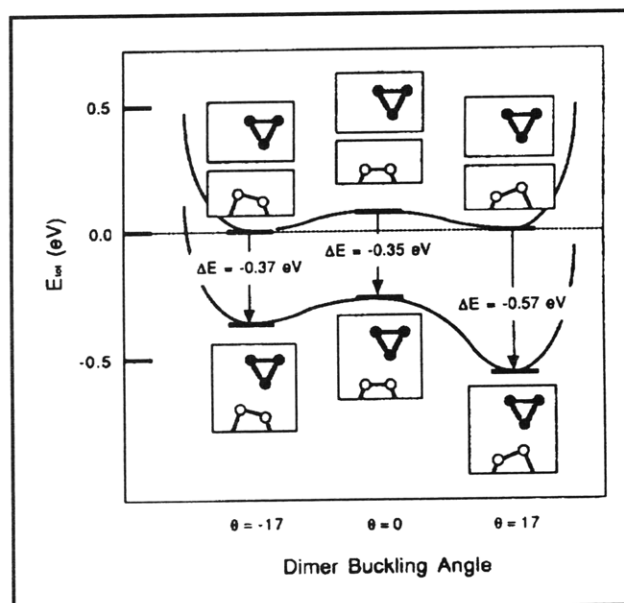

Figure 4. Total energy (in eV) of a tip-surface system as a function of surface-dimer buckling angle. The tip (shown schematically as a triangle with filled circles) is situated directly above a surface-dimer atom (open circles). The results at and above the horizontal dashed line correspond to $E(\text{tip}) + E(\text{surface})$. Note that the barrier for flipping from one asymmetric dimer configuration to the other is about 0.08 eV. The panels below the dashed line correspond to the fully interacting tip-surface system. In this case the horizontal bars correspond to $E(\text{tip} + \text{surface})$. Note that the barriers for up flip and down flip are 0.1 and 0.3 eV, respectively.

Implications. For a given value of energy barrier E_b, the average time that a dimer spends in one asymmetric configuration before flipping to the other is simply

$$\tau_b = 10^{-13} e^{E_b/k_B T},$$

where the phonon frequency is estimated to be 10^{13} sec^{-1}. During an STM measurement, an STM tip typically stays 2×10^{-3} sec $= t_{STM}$ above a surface atom, and therefore the relative values of τ_b and t_{STM} will determine the nature of the STM image. In the *absence of interactions* between the STM tip and the surface, a buckled dimer is in a symmetric potential well as shown in the upper curve of figure 4, and the energy barrier for flipping (0.08-0.09 eV) is small enough that at room temperature the dimer can flip up and down very frequently ($\tau_b = 2 \times 10^{-12}$ sec). This would lead to a symmetric STM image that is the average of up-flip and down-flop configurations.

In the presence of interactions between the STM tip and surface, a buckled dimer is an asymmetric potential well as shown in the lower curve of figure 4 and τ_b is different for the down-flip and the up-flip configurations. At room temperature, τ_b's are short enough ($\tau_{down} = 5 \times 10^{-12}$ sec and $\tau_{up} = 1.3 \times 10^{-8}$ sec) that, in principle, the dimer can flip up and down freely, and thermal equilibrium between two local energy minima of the asymmetric potential is reached during the STM imaging time. Therefore, the dimer spends different amounts of time in each local energy minimum, and the ratio of the times is given by the Boltzmann factor of the difference of two local minimum energies (4×10^{-4}). Consequently, the dimer stays in the up-flip configuration except for intermittent rapid round trips to the down-flip configuration. For all practical purposes, therefore, one is always measuring a dimer in the up-flip position as the tip moves along the surface. The resulting image is then deceptively that of a "symmetric" dimer.

2.4 Publications

Arias, T., and J.D. Joannopoulos. "Electron Trapping and Impurity Segregation at Grain Boundaries." *Phys. Rev. B* 49: 4525 (1994).

Arias, T., and J.D. Joannopoulos. "Ab-initio Theory of Dislocation Interactions." *Phys. Rev. Lett.* 73: 680 (1994).

Brommer, K., M. Calvan, A. Dal Pino, and J.D. Joannopoulos. "Theory of Adorption of Atoms and Molecules on Si(111)-(7x7)." *Sur. Sci.* 314: 57 (1994).

Capaz, R., A. Dal Pino, and J.D. Joannopoulos. "Identification of the Migration Path of Interstitial Carbon in Si." *Phys. Rev. B* 50: 7439 (1994).

Cho, K., and J.D. Joannopoulos. "The Devilish World of Surfaces." *Proceedings of the Teraflop Computer Conference*, Baton Rouge, 1994.

Devenyi, A., K. Cho, T. Arias, and J.D. Joannopoulos. "Adaptive Riemannian Metric for All-Electron Calculations." *Phys. Rev. B* 49: 13373 (1994).

Fan, S., A. Devenyi, R. Meade, and J.D. Joannopoulos. "Guided Modes in Periodic Dielectic Materials." *J. Opt. Soc. Am.* (1995) in press.

Fan, S., P. Villeneuve, R. Meade, and J.D. Joannopoulos. "Design of 3D Photonic Crystals at Submicron Lengthscales." *Appl. Phys. Lett.* 65: 1466 (1994).

Joannopoulos, J.D., "Ab-initio Statistical Mechanics." *Proceedings of the QTRM Conference*, Berkeley, California, 1994.

Larrabee, J., V. Baisley, R. Huffman, R. Meade, and J.D. Joannopoulos. "Detectivity of a UB-B Photodiode." *Proceedings of the SPIE Conference*, San Diego, California, 1994.

Meade, R., A. Devenyi, J.D. Joannopoulos, O. Alerhand, D. Smith, and K. Kash. "Novel Applications of Photonic Band Gap Materials." *J. Appl. Phys.* 75: 4753 (1994).

Mucciolo, E., R. Capas, B. Altshuler, and J.D. Joannopoulos. "Manifestation of Quantum Chaos in Electronic Band Structures." *Phys. Rev. B* 50: 8254 (1994).

Winn, J., R. Meade, and J.D. Joannopoulos. "Two Dimensional Photonic Band Gap Materials." *J. Opt.* 41: 257 (1994).